

The Effect of an Alcohol Resistant Aqueous Film Forming Foam (AR-AFFF) on the Evaporation, Boiling, and Collision Dynamics of a Water Droplet on a Heated Solid Surface¹

Samuel L. Manzello² and Jiann C. Yang

Building and Fire Research Laboratory, National Institute of Standards and Technology, Gaithersburg, Maryland 20899

Received March 6, 2002; accepted July 15, 2002

An experimental study is presented for droplets containing an alcohol-resistant aqueous film forming foam (AR-AFFF) impacting and boiling on a heated stainless steel surface. Experiments with solutions of 3% (volume fraction) AR-AFFF/distilled water were compared to ones with distilled water and 3% AR-AFFF/simulated seawater. The latter experiments were motivated by the practice of mixing AR-AFFF with seawater in many naval applications. The impact process was recorded using a high-speed digital camera at 1000 frames per second. For each fluid, the droplet impact Weber number was fixed, and the droplet evaporation lifetime was measured as a function of temperature. Collision dynamics were investigated for each fluid, with the temperature of the stainless steel surface varied from film evaporation to film boiling. It was observed that the addition of 3% AR-AFFF to water reduced the temperature for departure from nucleate boiling and the Leidenfrost temperature dramatically compared to pure water. Droplets were observed to breakup violently for solutions of AR-AFFF/simulated seawater at film boiling. The results demonstrate that the collision dynamics depend on what type of water is mixed with AR-AFFF. © 2002 Elsevier Science (USA)

Key Words: droplet; impact; heated surface; boiling.

INTRODUCTION

Firefighting foams have been used to combat a variety of flammable liquid fires (1). Application of firefighting foams to a pool fire results in the generation of a foam on the liquid surface. The presence of the foam acts to cool the fuel surface and prevent the fuel vapor from reaching the flame front, leading to fire extinguishment. Protein-based foam compounds were the first foaming agents put to use. These compounds are synthesized from hydrolysis products of protein containing matter such as hoof meal, chicken feathers, and fish meal (2).

The ability of firefighting foams to suppress pool fires was greatly advanced with the proliferation of aqueous film form-

ing foams (AFFF) (1). AFFF compounds contain synthetically produced fluorinated surfactants. The degree to which a given surfactant can lower the surface tension of a solution is dependent on the selective adsorption of the surfactant on the liquid/air interface (2). The amount of adsorption is dependent on the hydrophilic component and the hydrophobic component of the surfactant. The hydrophobic component is most often a hydrocarbon (2). In fluorinated surfactants, fluorine is present in the hydrophobic component. The addition of fluorine to the hydrophobic component allows a fluorinated surfactant to resist a variety of fats and oils (2). Additionally, fluorinated surfactants can lower surface tension dramatically compared to surfactants where the hydrophobic component is a hydrocarbon. The reduced surface tension and oil repellent nature of fluorinated surfactants present in AFFF allow it to spread over a hydrocarbon pool fire.

Alcohol-resistant aqueous film forming foam (AR-AFFF) compounds represent a further improvement to AFFF compounds. AR-AFFF foams are predicated on chemistry similar to that of AFFF compounds (i.e., the presence of fluorinated surfactants) with the addition of a synthesized polymer. Such polymers allow the foam to form a layer that encases it from the fuel. As a result, AR-AFFF compounds can be applied to fires where the fuel is miscible with water (e.g., alcohols). Consequently, AR-AFFF foams are the most widely used foaming agents.

To use AR-AFFF it is necessary to mix it with water. After the AR-AFFF is mixed with water, application of the agent to the fire is usually achieved in the form of droplets (3). Studies using water mist fire suppression systems have reported that a large fraction of the water droplets do not penetrate the fire since the droplet momentum is so small that the droplets can be directed away from the rising fire plume (4). King *et al.* (5) suggest that these deflected droplets impinge upon heated surfaces near the fire and ultimately evaporate. These droplets can still act to suppress the fire since evaporating droplets provide surface cooling of nearby heated surfaces and the vapor from these evaporating droplets may ultimately be entrained into the fire leading to extinguishment. Therefore, understanding droplet impact upon heated surfaces can have implications upon fire suppression.

¹ Official contribution of the National Institute of Standards and Technology not subject to copyright in the United States.

² National Research Council (NRC) Post-Doctoral Fellow. To whom correspondence should be addressed. E-mail: Samuel.Manzello@nist.gov.

Under practical conditions, the dispersion of the liquid agent results in the generation of numerous droplets that can be difficult to study systematically. A simpler approach can be adopted to understand the influence of droplet impingement on a heated surface. One such approach used is the study of single droplet impingement upon heated surfaces.

The impact of a liquid droplet with a solid surface can result in droplet spread, splash, or rebound (6). Whether a droplet will spread, splash, or rebound is dependent upon the droplet velocity, surface temperature, and surface roughness (7). In droplet impact experiments at room temperature, Mundo et al. (7) reported that whether a droplet will spread or splash depends upon the Ohnesorge (**Oh**) number, Reynolds (**Re**) number, and surface roughness. The **Oh** and **Re** numbers are defined as

$$Oh = \frac{\mu}{\sqrt{\rho\sigma D}} \quad [1]$$

$$Re = \frac{\rho V D}{\mu}, \quad [2]$$

where μ is the liquid viscosity, ρ is the liquid density, V is the impact velocity of the droplet, D is the initial droplet diameter, and σ is the equilibrium surface tension. The **Oh** number is the ratio of viscous to surface tension forces, and the **Re** number measures the ratio of inertial to viscous forces. Another parameter used to quantify the impact energy is the droplet **We** number (6). The **We** number, which is the ratio of droplet inertia to surface tension forces, is defined as

$$We = (Oh Re)^2 = \frac{\rho V^2 D}{\sigma} \quad [3]$$

where all properties are identical to those defined in Eqs. [1] and [2]. The **We** number has been used extensively to characterize droplet impact regimes on heated surfaces (8–10). While the **We**, **Oh**, and **Re** numbers are used extensively in droplet impact studies, it is important to note that other dimensionless groups may become important depending upon the impact conditions (7).

Droplet impact upon heated surfaces introduces additional complexities (9). Understanding the influence of surface temperature on droplet collision dynamics for a particular fluid requires the mapping of various boiling regimes. The droplet evaporation lifetime as a function of surface temperature can be used to delineate different heat transfer regimes, thus providing a mechanism to better understand the influence of surface temperature on droplet collision dynamics (11, 12). For a droplet gently deposited on a surface, the total droplet evaporation lifetime will decrease with increasing surface temperature until a minimum evaporation lifetime is obtained. The minimum evaporation lifetime marks the departure from nucleate boiling. After the minimum evaporation lifetime is reached, the total evaporation lifetime of the droplet will begin to rise with surface temperature. The Leidenfrost temperature occurs where the total evaporation lifetime of the droplet reaches a local maximum.

For temperatures greater than the Leidenfrost temperature (film boiling regime), the droplet evaporation lifetime will monotonically decrease with further increases in surface temperature.

Manzello and Yang (13) performed a thorough review of literature pertaining to water droplet impact on heated surfaces. Although significant work has been performed for water droplet impact on heated surfaces, few studies have addressed additives relevant to fire suppression (5, 13, 14). Specifically, to the authors' knowledge, no studies exist for *single* AR-AFFF droplets impacting upon a heated solid surface.

Results of the literature survey uncovered that work is available for droplets containing surfactants impacting on unheated surfaces (15–17). However, sparse literature is available for droplets containing surfactants impacting on heated surfaces.

Qiao and Chandra (18) considered the impact of droplets on a heated stainless steel surface. The surfactant used in their experiments was sodium dodecyl sulfate, and the concentration was varied from 0.01 to 0.1% (mass fraction). All droplets were 2.0 mm in initial droplet diameter and were released from a distance of 50 mm. The addition of 0.1% sodium dodecyl sulfate reduced the surface tension of water droplets from 0.073 to 0.050 N/m at 20°C. It was reported that the addition of this surfactant at 0.1% produced a 50°C reduction in the measured Leidenfrost temperature. The temperature at which departure from nucleate boiling occurred remained the same with or without the presence of surfactant. Sodium dodecyl sulfate is not a fluorinated surfactant (19). Fluorinated surfactants, used in fire suppression applications, are known to result in lower surface tension compared to surfactants such as sodium dodecyl sulfate that contain a hydrophobic component composed of hydrocarbons (2).

In this investigation, an experimental study of droplet/surface interaction was performed using droplets containing 3% (volume fraction) AR-AFFF. AR-AFFF was selected in this study since it is widely used in fire suppression applications. A concentration of 3% AR-AFFF was selected in accordance with the UL 162 Standard for AR-AFFF (20) and AR-AFFF mixtures for fresh water and seawater. Extensive testing has shown that 3% AR-AFFF is effective in fire mitigation. The AR-AFFF was mixed in concentrations of 3% (volume fraction) with water and simulated seawater. The latter experiments have been motivated by the practice of mixing AR-AFFF with seawater in many naval applications. A complication with real seawater is that it contains a great deal of impurities, in addition to salt, and these impurities vary depending on the sampling location (21). Therefore, simulated seawater (3.5% mass fraction NaCl) (21) was used. This reduced the uncertainty as to what constituents the droplets contained. The droplet evaporation lifetime was obtained as a function of surface temperature to delineate various heat transfer regimes for the 3% AR-AFFF solutions of distilled water and simulated seawater. The collision dynamics were examined within the nucleate boiling, transition boiling, and film boiling regimes. Finally, distilled water droplets were used for direct comparison with the 3% AR-AFFF solutions.

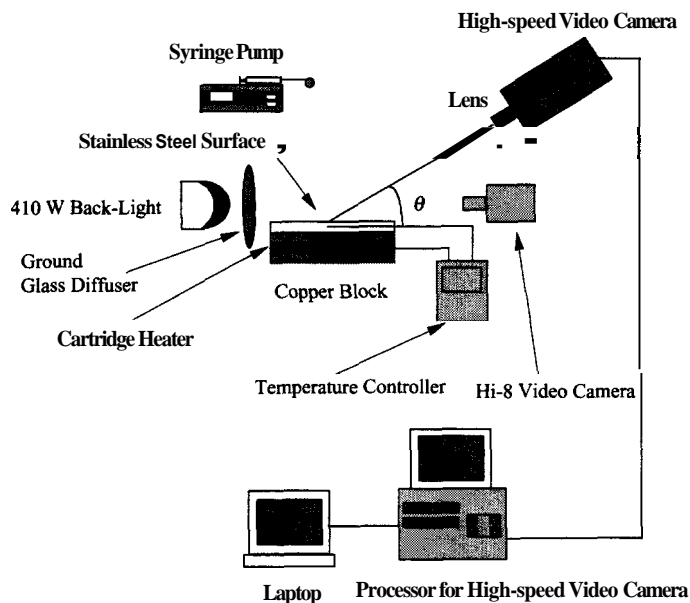


FIG. 1. Schematic of the experimental setup used for the droplet impact study. The figure shows the syringe pump, stainless steel surface, high-speed camera, and imaging optics.

MATERIALS AND METHODS

Figure 1 is a schematic of the experimental setup. All droplets were generated using a Yale³ YA-12 syringe pump programmed to dispense the liquid at a rate of 0.001 mL/s. The droplet was formed at the tip of the needle (25 gauge) and detached from the syringe under its own weight. The impacting droplet temperature for each solution was fixed at 20°C. To measure the droplet evaporation lifetime, droplets were gently placed on a rectangular stainless steel surface (SS 304), 3 cm wide, 5 cm long, and 0.5 cm thick. The stainless steel surface was polished based upon the recommendations of previous work (9). Sand paper (600 grit) was first used to polish the surface with subsequent application of metal polish to create a mirror finish. Surface heating was accomplished using a copper block with two miniature cartridge heaters embedded within it. The surface temperature was measured using a thermocouple embedded within the stainless steel surface. The location of the thermocouple was centered within the block and inserted 1 mm below the surface. It must be noted that all temperatures reported in this study correspond to those measured in the solid. Measuring the temperature at the surface is difficult. For this reason, many studies report surface temperatures that are actually measured close to the surface but within the solid (9). Chandra and Avedisian (9) used a stainless steel surface and measured the temperature 0.8 mm below the surface with a thermocouple, similar to the present experimental

³ Certain commercial equipment is identified in this paper in order to accurately describe the experimental procedure. This in no way implies recommendation by National Institute of Standards and Technology.

measurements. They estimated that the actual surface temperature was within 1°C of the measured temperature within the steel. Based on the similarities between the present experiments and those of Chandra and Avedisian (9), it is assumed that the surface temperature in this study is within 1°C of the measurement made within the stainless steel. The surface temperature was controlled to within $\pm 1^\circ\text{C}$ using a temperature controller. A CCD camera (with a framing rate of 30 frames per second) was used to measure the droplet evaporation lifetime.

Droplet impact dynamics were imaged using a Kodak EktaPro 1000 HRC digital high speed camera at 1000 frames per second with shutter speed set to 50 μs . The camera was fitted with a Nikon 60-mm micro lens to obtain the required spatial resolution to capture droplet impact. The camera was aligned at an angle $\theta = 33^\circ$ with respect to the horizontal. The light source used for backlighting was found to be the most important parameter that influenced the image quality of the collision dynamics. If the backlight was too dim, the collision dynamics were barely visible. A very bright backlight resulted in the converse problem, image saturation. One 410-W floodlight bulb (see Fig. 1) proved to be the optimal light source. The light source was kept as far away from the test surface as possible to mitigate heating of the droplet and stainless steel surface. A distance of 0.2 m proved to be the furthest location from the impact site that uniform illumination could be maintained. The light source was turned on the moment the droplet was released from the syringe and was switched off after droplet impact. The total time the light was on was no more than ≈ 2 s per experiment; thus it is not expected that the presence of the light influenced the collision dynamics by heating of the droplet and the surface. A ground glass diffuser was placed in front of the light source to provide more uniform illumination of the stainless steel surface.

The impact velocity was measured by tracking the location of the droplet centroid 1 ms prior to impact using the Scion image processing software. The initial droplet diameter was determined 2 ms prior to impact. The image processing software was used to threshold the droplet from the background and the diameter of the droplet was measured both in the horizontal and the vertical direction. The difference in the diameter measured in the vertical and the horizontal direction was at most 0.3 mm. The droplet diameter was defined as the average of the two measurements. The computer system was used to store the digital images for subsequent analysis (see Fig. 1).

Chandra and Avedisian (9) used single shot photography to provide beautiful pictures of droplet collision dynamics. In single shot flash photography, droplet collision dynamics are constructed from an ensemble of photographs of individual droplets impacting the surface at different times. In many subsequent publications, the technique was honed to capture droplet impact, from molten metals to surfactant-laden droplets (18, 22). Their justification for using the single shot method was predicated on the poor quality of images obtained from high-speed cameras in the past. Using the current setup, we are able to capture droplet impact clearly using a digital high-speed camera. An

advantage of the high-speed technique is that the same droplet is followed during the impact process. The temporal resolution of the high-speed photographs in this study was limited to 1 ms, the framing rate of the camera. Other investigations have used high-speed cameras with greater temporal resolution (23, 24). For example, in their study of satellite droplet dynamics, Notz *et al.* (24) used a digital imaging system capable of storing eight images with interframe and exposure times to 10 ns.

National Foam Universal Gold AR-AFFF was used for the experiments. This type of AR-AFFF contained water, a proprietary fluorinated surfactant, polysaccharide, 2-methoxymethylethoxy propanol, and a proprietary mixture of synthetic detergents. The AR-AFFF was mixed in concentrations of 3% (volume fraction) with water and simulated seawater.

The liquid density for 3% AR-AFFF mixed with distilled water and simulated seawater was measured to be 981 ± 4 and $1002 \pm 9 \text{ kg m}^{-3}$, respectively (mean \pm standard deviation). The surface tension was measured using a CSC Scientific 70535 Du Nouy tensiometer. The value of surface tension obtained for 3% AR-AFFF with distilled water and simulated seawater was measured to be 0.0235 ± 0.004 and $0.022 \pm 0.004 \text{ N/m}$, respectively. All properties were measured at 20°C .

RESULTS AND DISCUSSION

Figure 2 displays the droplet evaporation lifetime as a function of surface temperature for 3% AR-AFFF/distilled water with initial diameter of $2.4 \pm 0.1 \text{ mm}$ (mean \pm standard deviation). The droplet evaporation lifetime was recorded in 10°C intervals

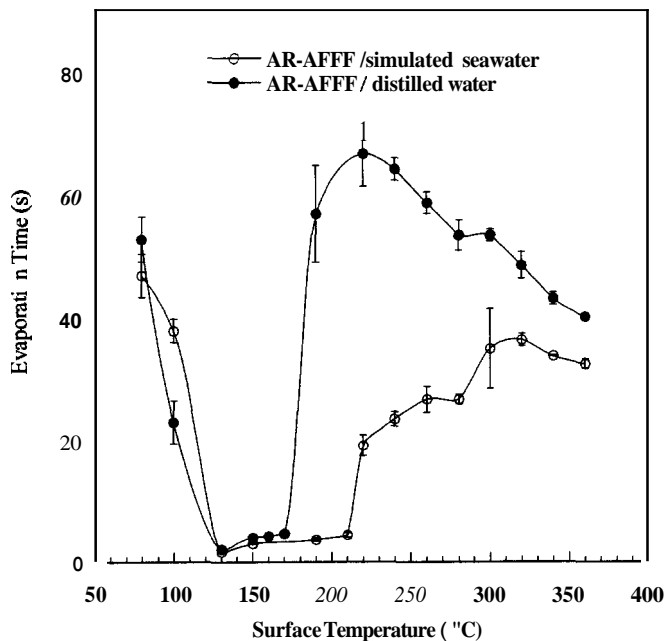


FIG. 2. Measured evaporation lifetime for droplets containing 3% AR-AFFF mixed with water and simulated seawater.

with a reduced interval of 5°C near the minimum evaporation lifetime and the Leidenfrost temperature. At each temperature three sequential experiments were performed and the evaporation time at each temperature represents the average of the three tests with the error bars representing the standard deviations of the measurements (mean \pm standard deviation).

The parameters influencing the uncertainty in determining the temperature of the minimum evaporation lifetime and the Leidenfrost temperature were the droplet evaporation lifetime, the measured temperature of the surface, and the temperature interval at which the evaporation lifetime was measured. As pointed out by Bernardin and Mudawar (25), the uncertainty in the droplet evaporation lifetime is greatly reduced by averaging over several experiments. Thus, the measured temperature of the surface and the temperature interval used to obtain the evaporation lifetime are believed to be the dominant factors influencing the measurement uncertainty. With the surface temperature controlled to within 1°C and using a 5°C interval, the uncertainty in determining the Leidenfrost temperature and temperature for departure from nucleate boiling was estimated to be $\pm 12^\circ\text{C}$.

From Fig. 2, the minimum evaporation lifetime for 3% AR-AFFF/distilled water droplets was measured to occur at a temperature of 130°C . The Leidenfrost temperature was measured to be 220°C . Transition boiling will occur from 130 to 220°C , with film boiling above the Leidenfrost temperature (220°C).

The droplet evaporation lifetime was also obtained as a function of surface temperature for 3% AR-AFFF/simulated seawater (see Fig. 2). The initial droplet diameter was $2.4 \pm 0.1 \text{ mm}$.

A complication when working with dissolved solids in an aqueous solution is the presence of solid residual formed when attempting to measure the droplet evaporation lifetime (5). The total evaporation lifetime was defined in a manner similar to that of King *et al.* (5) as the time the solid residual droplet appeared minus the time the droplet was placed upon the surface. Three percent AR-AFFF/simulated seawater resulted in an increase in the Leidenfrost temperature compared to 3% AR-AFFF/distilled water. The measured Leidenfrost temperature for 3% AR-AFFF/simulated seawater was 320°C . The temperature for departure from nucleate boiling was not affected, it was the same for both 3% AR-AFFF solutions.

Results obtained for the 3% AR-AFFF solutions were compared with those obtained for distilled water. Figure 3 displays the measured evaporation lifetime as function of surface temperature for distilled water droplets of $2.7 \pm 0.1 \text{ mm}$ in initial diameter. Qualitatively, the curve is similar in shape to solutions containing 3% AR-AFFF. From Fig. 3, the surface temperature for departure from nucleate boiling was measured to be 230°C . The Leidenfrost temperature was measured to be 330°C . Within experimental uncertainty, the measured Leidenfrost temperature was similar for distilled water and 3% AR-AFFF/simulated seawater. Additionally, the Leidenfrost temperature measured for distilled water droplets on stainless steel matched values reported in the literature (12). It is important to note that although

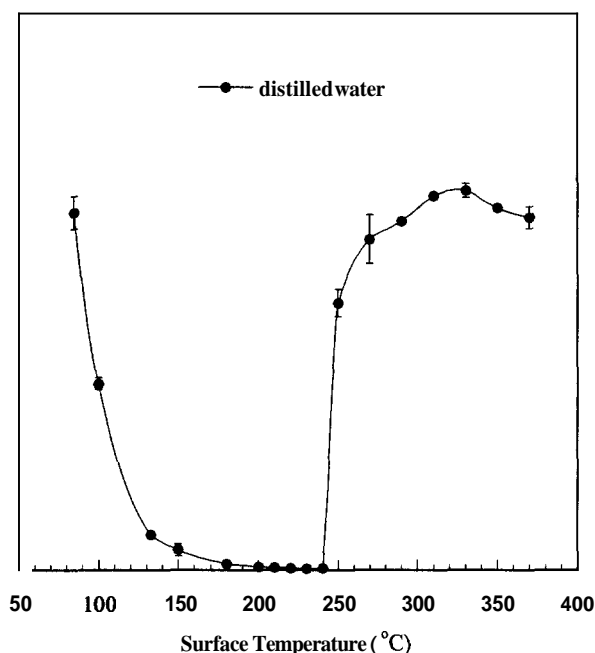


FIG. 3. Measured evaporation lifetime for distilled water droplets.

the initial droplet size was slightly larger for distilled water droplets than for the 3% AR-AFFF solutions (2.7 mm vs 2.4 mm), the Leidenfrost temperature for distilled water is known to be independent of initial droplet size (12, 25, 26).

The addition of 3% AR-AFFF to distilled water and simulated seawater resulted in differences in the Leidenfrost temperature and the temperature for departure from nucleate boiling compared to distilled water. Qiao and Chandra (18) observed that the Leidenfrost temperature was greatly reduced as small concentrations of surfactant were added to water droplets. In their experiments, it was observed that the droplet evaporation lifetime increased for droplets containing surfactant in the transition boiling regime. It was believed that changes in the droplet evaporation lifetime for surfactant-containing droplets were the result of suppression of the miniaturization phenomena observed by Inada and Yang (27).

Inada and Yang (27) delineated the mechanics of a phenomenon termed “miniaturization” for water droplets on a heated surface. Miniaturization was defined as the expulsion of minute droplets from the surface of the droplet after deposition on a heated surface. Water droplets impacted a heated platinum surface and measurements of the frequency and amplitude of elastic-longitudinal waves produced from boiling were monitored. Measurements of the acoustic pressure of the boiling droplets were also measured using a microphone. Surface temperatures within the transition boiling regime resulted in the maximum magnitude and frequency of elastic-longitudinal waves and the largest acoustic pressure. Miniaturization was strongest within the transition boiling regime but “miniaturization” was also observed slightly below the transition boiling regime.

Inada and Yang (27) believed miniaturization was due to the generation of vapor bubbles within the liquid film. The vapor bubbles grow and eventually break through the surface, resulting in “many liquid clusters that burst through the liquid film surface like multiple firecrackers.” Qiao and Chandra (18) speculated that the greater evaporation lifetime within the transition boiling regime for surfactant-containing droplets shifted the evaporation lifetime curve, producing a Leidenfrost temperature lower than that of distilled water droplets.

A similar argument may describe differences in the measured Leidenfrost temperature for the 3% AR-AFFF solutions. When 3% AR-AFFF/simulated seawater droplets impacted the surface, vigorous miniaturization was observed. For droplets containing 3% AR-AFFF/distilled water, miniaturization was suppressed compared to 3% AR-AFFF/simulated seawater droplets. For AR-AFFF droplets containing simulated seawater, as the droplet evaporated, a residue of salt was produced. It is known that the presence of the salt residue may provide more nucleation sites (28), resulting in vigorous miniaturization compared to AR-AFFF mixed with distilled water.

The influence of enhanced miniaturization in the transition boiling regime can clearly be seen in Fig. 2. Within transition boiling, droplets containing 3% AR-AFFF/simulated seawater resulted in a shorter evaporation lifetime compared to droplets of 3% AR-AFFF/distilled water. The reduction in the droplet evaporation lifetime within the transition boiling regime shifted the location of the Leidenfrost temperature to higher temperatures for 3% AR-AFFF/simulated seawater droplets.

Even though the initial droplet size was larger for water (2.7 mm) than for the AR-AFFF solutions (2.4 mm), the total evaporation lifetime was much shorter for water droplets at departure from nucleate boiling. Indeed, extremely vigorous miniaturization was observed for water droplets. Consequently, it is not surprising that distilled water droplets resulted in a Leidenfrost temperature similar to that of droplets containing 3% AR-AFFF/simulated seawater.

A variety of correlations are available for prediction of the Leidenfrost temperature (25). A widely used correlation, proposed by Baumeister and Simon (29), requires fluid property data such as the critical temperature. Such information is not available for AR-AFFF solutions. Bernardin and Mudawar (25) point out that other available correlations require various other fluid properties (e.g., enthalpy of vaporization). Estimation of these properties is complicated since the constituent components that compose AR-AFFF are proprietary. Thus, it was not possible to compare the measured Leidenfrost point with such correlations in the present study.

Figure 4 displays temporally resolved images of 3% AR-AFFF/distilled water droplet impact upon a stainless steel surface at 100, 130, and 220°C for an impact We number of 185. The impact We number was calculated from thermophysical properties measured at 20°C. For fire suppression applications, the impacting droplets are not expected to have low impact We numbers (30). Consequently, in this investigation, the impact

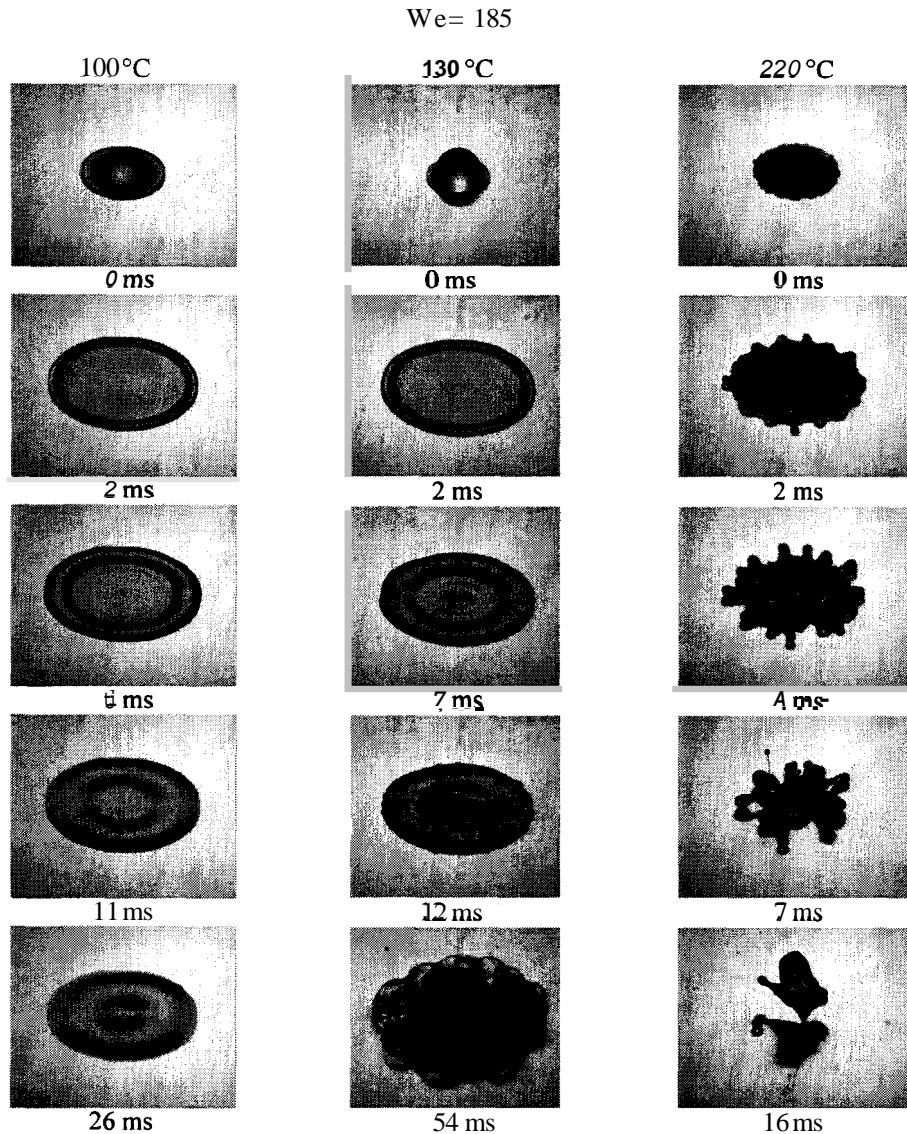


FIG. 4. Temporal variation of 3% AR-AFFF/distilled water droplet impact on a heated stainless steel surface. The three panels display droplet impact for surface temperatures of 100, 130, and 220°C.

velocity (thus We number) was selected to produce inertial forces two orders of magnitude larger than surface tension forces. Since each experiment displayed similar qualitative trends, results of three consecutive experiments were used for data analysis.

Collision dynamics at the temperature for departure from nucleate boiling (130°C) were unlike those at 100°C (see Fig. 4). At a time of 7 ms after impact, the onset of boiling was observed. As time progressed, vigorous foaming ensued.

Droplet impact at the Leidenfrost temperature (220°C) for 3% AR-AFFF/distilled water droplets was distinct from those at 100°C and the departure from nucleate boiling. Immediately after impact, the droplet was observed to flatten into a disk. With increasing time, the liquid film began to contract and ultimately lifted off the surface at 16 ms. The surface temperature was

increased to arrive at temperatures within the film-boiling regime (250°C). The collision dynamics at film boiling were observed to be qualitatively similar to those at the Leidenfrost temperature.

Comparing the impact of 3% AR-AFFF/distilled water droplets with other solutions required matching the impact We number in addition to the boiling regimes. Matching the impact We number exactly is difficult since the We number is obtained from statistical averages of droplet diameter and impact velocity. The We numbers for water droplet impact and 3% AR-AFFF/simulated seawater droplet impact were equal to 171 and 184, respectively. These values are based on properties evaluated at 20°C. The relative standard uncertainty in determining the Weber number was $\pm 8\%$. Within experimental uncertainty, the We number was similar for all three fluids considered.

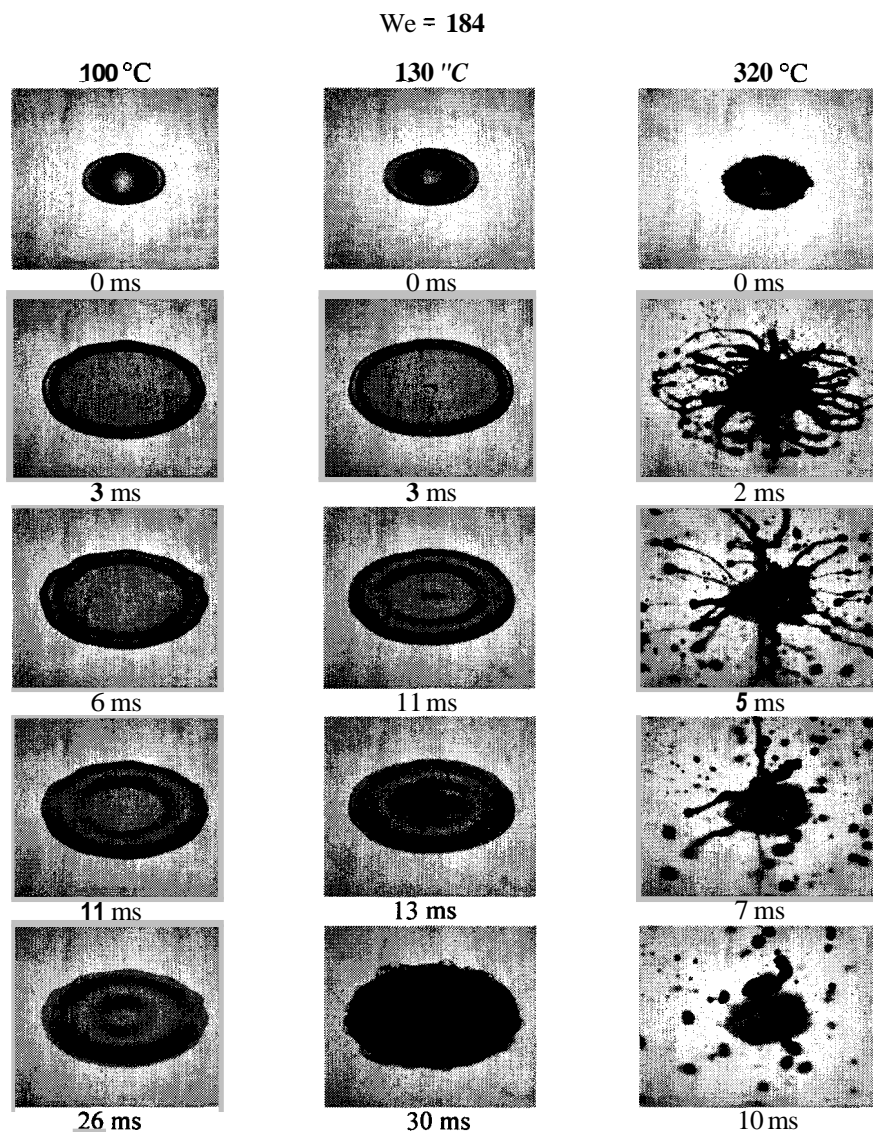


FIG. 5. Temporal variation of 3% AR-AFFF/simulated seawater droplet impact on a heated stainless steel surface. The three panels display droplet impact for surface temperatures of 100, 130, and 320°C.

Figure 5 displays time-elased images of 3% AR-AFFF/simulated seawater droplet impact at 100, 130, and 320°C for an impact We number of 184. Impact at departure from nucleate boiling (130°C) resulted in vigorous boiling with foaming, similar to what was observed for 3% AR-AFFF/distilled water. The collision dynamics at the Leidenfrost temperature, however, were dissimilar. For 3% AR-AFFF/simulated seawater, the droplet impacted the surface and disintegrated immediately upon impact. The salt precipitated from the solution and left a residue behind.

Distilled water droplet impact was compared to both 3% AR-AFFF solutions. Impact at 230°C is shown in Fig. 6. For distilled water, vigorous boiling was observed without the presence of foaming. At the Leidenfrost temperature (330°C), the droplet was observed to form a stable liquid film diameter for 1 ms

and then to disintegrate, similar to 3% AR-AFFF mixed with simulated seawater.

The evolution of the liquid film diameter with time is necessary to determine the portion of the surface undergoing cooling (10). The temporal variation of the liquid film diameter was measured as a function of surface temperature for both 3% AR-AFFF solutions and distilled water. Results obtained for both 3% AR-AFFF solutions are shown in Fig. 7. The nondimensionalized liquid film diameter, β , was defined as the instantaneous liquid film diameter divided by the initial droplet diameter. The nondimensionalized diameter was defined as the average of three measurements at each temperature with the error bars representing the standard deviations. This diameter was measured up to the time it reached the maximum value and/or disintegration.

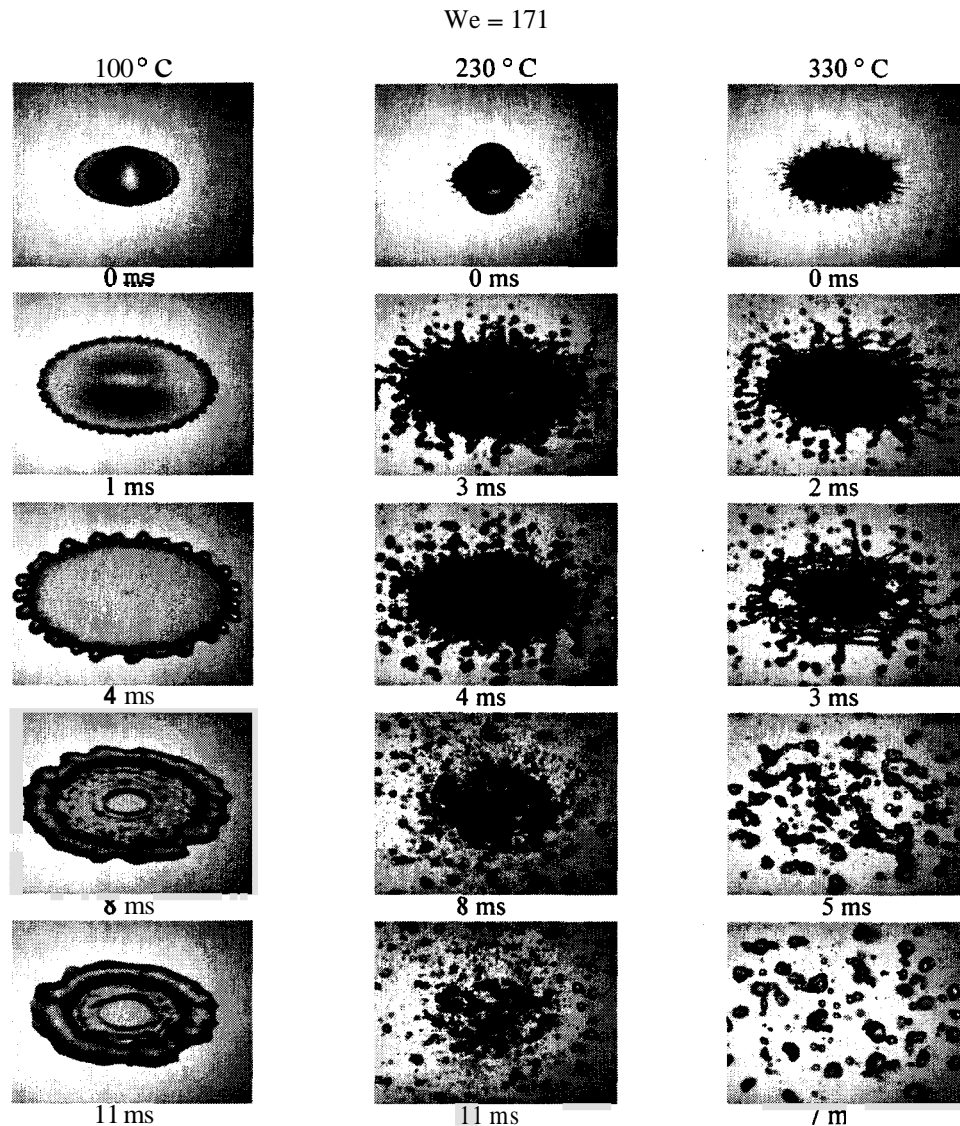


FIG. 6. Temporal variation of distilled water droplet impact on a heated stainless steel surface. The three panels display droplet impact for surface temperatures of 100, 230, and 330°C.

As shown in Fig. 7, β could not be measured for 3% AR-AFFF/simulated seawater at the Leidenfrost temperature and within film boiling due to the violent breakup. The nondimensionalized liquid film diameter was measured for 3% AR-AFFF/simulated seawater at 20°C, 100°C, and the temperature corresponding to the departure from nucleate boiling, 130°C. From these measurements, the 3% AR-AFFF mixtures containing simulated seawater provided a larger nondimensionalized liquid film diameter. Thus, at similar impact We number, 3% AR-AFFF/simulated seawater should provide a greater degree of surface cooling up to the departure from nucleate boiling. For surface temperatures above departure from nucleate boiling, 3% AR-AFFF/simulated seawater may also provide a greater degree of surface cooling due to the violent breakup. If the droplet

breaks up into several smaller droplets, a substantial increase will occur in the effective surface area with attendant increases in surface cooling compared to 3% AR-AFFF/water.

The temporal evolution of nondimensionalized liquid film diameter was also measured for distilled water and is displayed in Fig. 8. The maximum value of β for distilled water at 20 and 100°C was larger than measurements for 3% AR-AFFF solutions. For water, at 230, 330, and 350°C, β could not be measured past 1 ms due to instability of the liquid film. The disparity in the temporal evolution of the liquid film diameter for each fluid further reinforces the findings of Manzello and Yang (14). In that study, it was reported that even though the impact We number and boiling regimes were matched for different fluids, the evolution of liquid film diameter is different.

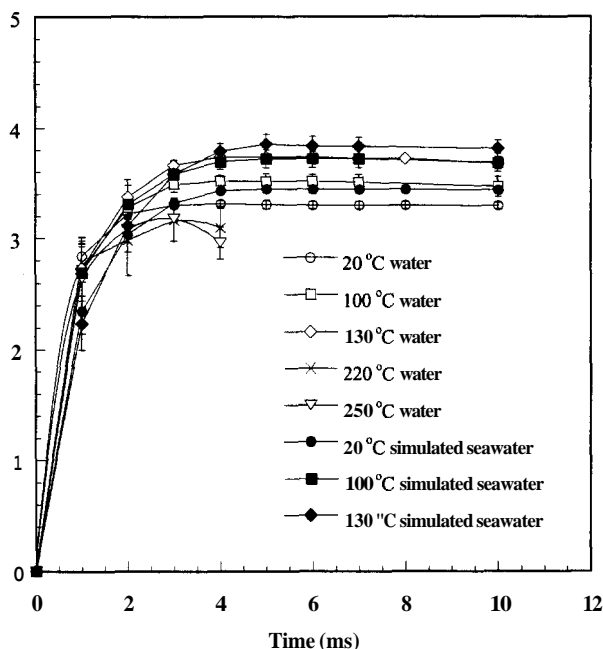


FIG. 7. Temporal variation of the measured liquid film diameter for various temperatures for 3% AR-AFFF solutions.

At the Leidenfrost temperature, 3% AR-AFFF mixed with pure water impacted, recoiled, and levitated (i.e., breakup was not observed) above the surface. Clearly, for the other fluids, the liquid film diameter was observed to breakup. These differences may be explained in terms of surface tension forces,

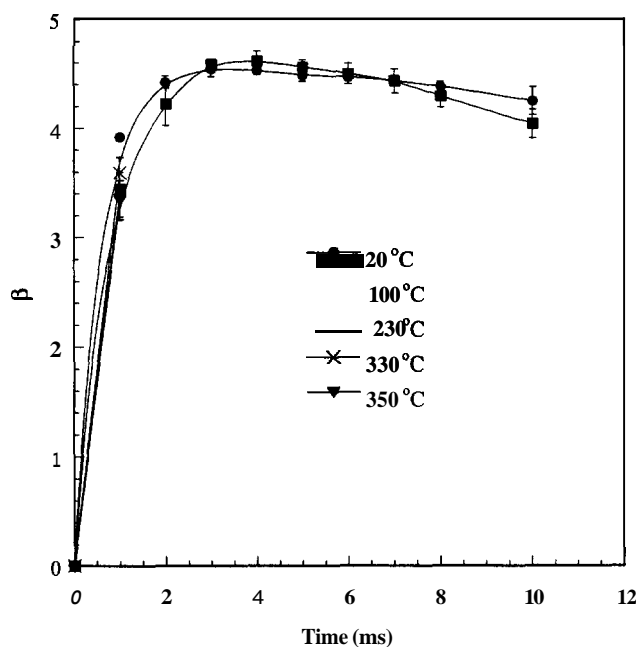


FIG. 8. Temporal variation of the measured liquid film diameter for various temperatures for distilled water droplet impact.

as the ability of the droplet to reform and recoil is believed to be due to surface tension (10). For 3% AR-AFFF/distilled water, the measured Leidenfrost temperature was reduced by 100°C compared to that of 3% AR-AFFF/simulated seawater. The measured surface tension was similar for both 3% AR-AFFF solutions at room temperature. Consequently, the surface tension forces of the 3% AR-AFFF/simulated seawater droplets are expected, at the Leidenfrost temperature, to be dramatically less than those of 3% AR-AFFF/distilled water droplets. Upon impact, 3% AR-AFFF/simulated seawater droplet is unable to regroup and violently shatters. It is assumed that the surface tension decreases as the surface temperature is increased for the AR-AFFF solutions. To the authors' knowledge, no published data for surface tension as a function of temperature for solutions of AR-AFFF are available. In future studies, the variation of surface tension with temperature for AR-AFFF solutions will be measured.

A similar conjecture can be made for distilled water droplet impact. Although the initial surface tension of distilled water is higher than that of both 3% AR-AFFF solutions, the Leidenfrost temperature for distilled water is similar to that for 3% AR-AFFF/simulated seawater. At all temperatures, the nondimensional liquid film diameter, β , was greater for distilled water than for the 3% AR-AFFF solutions. From conservation of mass, the liquid film diameter must be thinner for distilled water (for a fixed droplet size). With a thinner surface of liquid in contact with the heated surface, conduction of heat into the liquid film should be faster for distilled water, reducing surface tension dramatically. For distilled water, due to higher initial surface tension forces, the liquid film diameter was initially more stable than that of 3% AR-AFFF/simulated seawater.

Within film evaporation, (20°C), water droplets resulted in a larger liquid film diameter at similar impact We numbers. Zhang and Basaran (16) reported a qualitatively similar result. In their experiments, two different surfactants were used, namely, Triton X-100 and sodium dodecyl sulfate. For impact velocity greater than 1.6 m/s, water droplets were observed to have a liquid film diameter larger than that of droplets containing Triton X-100. They did not compute the impact We number, but with values of surface tension reported by Zhang and Basaran (16), the impact We number was estimated for the concentrations of Triton X-100. Based on these estimates, the liquid film diameter was greater for water at similar impact We number. Similar experiments were performed for droplets containing sodium dodecyl sulfate. However, for sodium dodecyl sulfate droplets, the liquid film diameter was always larger than that of water droplets for all concentrations considered.

Zhang and Basaran (16) explained these differences based on dilution of the surfactant due to interfacial dilatation or surface area creation. At high We number impact, the surface dilatation rate becomes large. The increase in the surface dilatation is thought to dilute the surfactant on the droplet interface and increase the instantaneous surface tension. An additional effect is that surfactant accumulates near the contact line due to the radial flow that ensues from the droplet impacting the surface.

These effects result in surface tension gradients along the interface that produce Marangoni stresses resulting in interfacial flow from the contact line to the drop center precluding droplet spread. The degree of the surface tension driven flow is dependent on the ability of the surfactant to occupy regions at the surface that are deficient in surfactant. They believed that increased spreading always occurred for sodium dodecyl sulfate since this surfactant was able to redistribute itself faster along the surface, mitigating the surface tension gradient. However, for Triton X-100, this was not the case and water was observed to spread more at similar impact We numbers. These arguments were supported by measurements of the dynamic surface tension of the surfactant-containing droplets. Measurements of dynamic surface tension showed that the rate of change of surface tension was considerably faster for sodium dodecyl sulfate than for Triton X-100.

If it is assumed that surfactants in the 3% AR-AFFF solutions are the controlling factor determining the collision dynamics, the results of Zhang and Basaran (16) suggest that the surfactant within AR-AFFF results in surface-tension-induced Marangoni stresses that preclude spreading resulting in larger β for distilled water than for AR-AFFF. Future studies must consider measuring the dynamic surface tension of the AR-AFFF solutions to fully answer these questions. Unfortunately, the heating of the solid surface and ultimate boiling of the liquid film greatly complicate the dynamics. Thus, their results can only be used to explain droplet spread under nonboiling conditions.

Comparisons with models that predict the evolution of liquid film diameter were not made. Manzello and Yang (13) reported minimal success with available models when comparing the evolution of liquid film diameter for water impact over a range of impact We numbers. Bernardin *et al.* (10) reported qualitatively similar findings for water droplets impacting upon a heated aluminum surface. Since these models are based on water impact and poor agreement was realized for water, it is not expected that good agreement would be obtained for solutions of 3% AR-AFFF.

SUMMARY

The results demonstrate that the degree of surface cooling depends on what type of water is mixed with 3% AR-AFFF. Three percent AR-AFFF/simulated seawater provides more coverage area and a reduced evaporation lifetime from film evaporation until departure from nucleate boiling compared with 3% AR-AFFF/distilled water. The combination of these effects suggests that application of 3% AR-AFFF/simulated seawater will wet more surface area with the surface area remaining wet longer than solutions of 3% AR-AFFF mixed with distilled water. This in effect should have a negative impact (i.e., beneficial for fire containment) on fire spread.

Within the film boiling regime, droplets were atomized immediately upon impact for 3% AR-AFFF solutions mixed with sim-

ulated seawater. For 3% AR-AFFF/distilled water, the droplet was never observed to breakup for the range of We numbers investigated. For 3% AR-AFFF/simulated seawater, film boiling began at much higher surface temperatures compared to 3% AR-AFFF/distilled water. The mixing of 3% AR-AFFF with distilled water or simulated seawater does not alter the temperature for departure from nucleate boiling nor the foaming ability of the mixture.

ACKNOWLEDGMENTS

S.L.M. acknowledges support from an NRC Post-Doctoral Fellowship. Mr. Derek Manzello of the National Oceanic and Atmospheric Administration (NOAA) is acknowledged for providing a suitable reference on the salinity of seawater. Two reviewers are acknowledged for providing comments invaluable to the integrity of the manuscript.

REFERENCES

1. Scheffey, J. L., Darwin, R. L., and Leonard, J. T., *Fire Technol.* **31**, 224 (1995).
2. Kissa, E., "Fluorinated Surfactants." Dekker, New York, 1994.
3. Pignato, J. A., *Fire Technol.* **19**, 5 (1983).
4. Downie, B., Polymeropoulos, C., and Gogos, G., *Fire Safety J.* **24**, 359 (1995).
5. King, M. D., Yang, J. C., Chien, W. S., and Grosshandler, W. L., in "Proceedings of the ASME National Heat Transfer Conference." Baltimore, MD, 1997.
6. Rein, M., *Fluid Dyn. Res.* **12**, 61 (1993).
7. Mundo, M., Sommerfeld, and Tropea, C., *Int. J. Multiphase Flow* **21**, 151 (1995).
8. Wachters, L. H., and Westerling, N. A. J., *Chem. Eng. Sci.* **21**, 1047 (1966).
9. Chandra, S., and Avedisian, C. T., *Proc. R. Soc. London A* **432**, 13 (1991).
10. Bernardin, J. D., Stebbins, C. J., and Mudawar, I., *Int. J. Heat Mass Transfer* **40**, 247 (1997).
11. Tamura, Z., and Tanasawa, Y., *Proc. Combust. Inst.* **7**, 509 (1959).
12. Xiong, T. X., and Yuen, M. C., *Int. J. Heat Mass Transfer* **34**, 1881 (1991).
13. Manzello, S. L., and Yang, J. C., *Proc. R. Soc. London A* **458**, 2026 (2002).
14. Manzello, S. L., and Yang, J. C., *Int. J. Heat Mass Transfer* **45**, 3961 (2002).
15. Cox, R. G., *J. Fluid Mech.* **168**, 195 (1986).
16. Zhang, X., and Basaran, O. A., *J. Colloid Interface Sci.* **187**, 166 (1997).
17. Mourougou-Candoni, N., Prunet-Foch, B., Legay, F., Vignes-Adler, M., and Wong, K., *J. Colloid Interface Sci.* **192**, 129 (1997).
18. Qiao, Y., and Chandra, S., *Proc. R. Soc. London A* **453**, 673 (1997).
19. Porter, M. R., "Handbook of Surfactants," 2nd ed. Chapman & Hall, London, 1994.
20. UL 162, "Standard for Foam Equipment and Liquid Concentrates," 7th ed. Underwriters Laboratories, Northbrook, IL, 1994.
21. Millero, F. J., "Chemical Oceanography," 2nd ed. CRC Press, Boca Raton, FL, 1996.
22. Aziz, S., and Chandra, S., *Int. J. Heat Mass Transfer* **43**, 841 (2000).
23. Kowalewski, T. A., *Fluid Dyn. Res.* **17**, 121 (1996).
24. Notz, P. K., Chen, A. U., and Basaran, O. A., *Phys. Fluids* **13**, 549 (2001).
25. Bernardin, J. P., and Mudawar, I., *J. Heat Trans.* **121**, 894 (1999).
26. Gottfried, B. S., Lee, C. J., and Bell, K. J., *Int. J. Heat Mass Transfer* **9**, 1167 (1966).
27. Inada, S., and Yang, W. J., *Int. J. Heat Mass Transfer* **36**, 1505 (1993).
28. Cui, Q., Chandra, S., and McCahan, S.; *J. Heat Transfer* **123**, 719 (2001).
29. Baumeister, K. J., and Simon, F. F., *J. Heat Transfer* **95**, 166 (1973).
30. Bolle, L., and Moureau, J. C., in "Multiphase Science and Technology" (J. D. Hewitt and N. Zuber, Eds.), pp. 1-92. Hemisphere, New York, 1981.

